Effects of wind on reservoir mixing and stratification: a case study from Kansas

by

Averi Baker

B.S., Kansas State University, 2022

A THESIS

submitted in partial fulfillment of the requirements for the degree

MASTER OF SCIENCE

Carl and Melinda Helwig Department of Biological and Agricultural Engineering
Carl R. Ice College of Engineering

KANSAS STATE UNIVERSITY
Manhattan, Kansas

2024

Approved by:

Major Professor
Dr. Trisha Moore

Copyright

Abstract

There is a growing concern of harmful algal blooms (HABs) in freshwater aquatic systems, including reservoirs throughout Kansas due to their toxicity and increased frequency. The impact of wind events on the stratification dynamics within reservoirs has been proven to greatly affect the surrounding environment, including mixing dynamics within reservoirs and conditions for HABs to form. This research study used the well-established General Lake Model (GLM), a one-dimensional hydrodynamic model, to analyze the effects of different wind scenarios on stratification and potential for harmful cyanobacterial blooms in Marion Reservoir. The GLM model was calibrated and verified using temperature profile data collected from Marion Reservoir in 2022 and 2023. Wind scenarios reflecting potential changes in wind speed during the algal bloom season were then applied in the model to examine the effects of wind on reservoir mixing dynamics. This research exemplifies the crucial impact of wind magnitude on stratification of lakes and reservoirs. These results further show the complex relationship between wind events and reservoir mixing.

Table of Contents

List of Figures

List of Tables

Chapter 1 - Introduction

The environmental concern of damage to ecological and economic sustainability of freshwater ecosystems from harmful algal blooms (HABs), specifically cyanobacterial blooms, has continued to rise in recent years. Cyanobacteria, often referred to as blue-green algae, are photosynthetic bacteria that produce toxins that result in harm to human and animal life in affected waters. These blooms are caused by increased nutrient inputs from human activities such as industrialization, urbanization, and agriculture. The development of HABs is impacted by various environmental conditions and physical factors. Warming climate plays a big role in the current trend of increasing bloom events around the world. Higher temperatures and radiation and decreasing wind speed causes earlier-occurring and longer-lasting HABs in warmer months [1]. As the climate continues to change, it will remain crucial to better understand the relationship between HABs and the surrounding environmental conditions that lead to them.

Wind is an important aspect of climatic effects on lakes and reservoirs, and, compared to the effects of temperature, it is less often studied. Wind plays an important role in the internal mixing dynamics of waterbodies, as higher wind speeds can overcome the effects of thermal stratification and induce mixing throughout the water column. Stratification itself is a well-studied piece of the puzzle and limits vertical mixing [2]. Intense vertical stratification can contribute to the growth of HABs and their proliferation at the surface under low-wind conditions [3]. Previous work has demonstrated that reduced wind speeds, known as atmospheric stilling, along with increased high wind events, likely influence stratification dynamics deeply [4]. As stated, wind plays a big part in lake mixing and stratification. These interactions in lakes and reservoirs greatly influence the entire ecosystem's functioning, especially nutrient cycling and potential HABs. In a study done at Rappbode Reservoir (Germany), the effect of different wind conditions on stratification was determined using the General Lake Model (GLM) [4]. Using various scenarios of wind speeds/patterns, the sensitivity of the stratification in the reservoir was analyzed. The results of the study showed that with increased wind speed, stratification duration and intensity were reduced, particularly when strong wind events occurred early in summer [4]. The sensitive time window of thermal dynamics to episodic wind events is demonstrated in this research.

The goal of this study is like that of the study at Rappbode Reservoir: to assess the sensitivity of stratification and lake mixing in Marion Reservoir in central Kansas to changing wind speed using a reliable, one-dimensional hydrodynamic model. In addition, this work aims to explore potential relationships between wind-driven mixing patterns and the onset of cyanobacterial blooms in Marion Reservoir. This work builds on previous trend analyses of historical wind data at Marion Reservoir by Rahmani and Bhandari (unpublished data). The GLM hydrodynamic model was used in this research because it represents the different meteorological and hydrological factors to provide robust predictions and reservoir hydrodynamic conditions [5]. The specific objectives of this thesis were to:

(1) develop and calibrate the 1-dimensional General Lake Model (GLM) for Marion Reservoir to simulate wind-driven mixing and thermal stratification,

(2) apply wind scenarios representing both uniform increases in windspeed and patterns representing increased variability in wind speed as episodic high wind – low wind sequences and assess potential changes in reservoir mixing, and

(3) examine relationships between observed cyanobacterial blooms and simulated lake mixing metrics.

This thesis is organized as follows: Chapter 2 provides a complete literature review; Chapter 3 details the methods by which the GLM model and wind scenarios were developed and assessed; Chapter 4 presents the results of calibration, wind scenario model runs, and analysis of associated reservoir mixing metrics; Chapter 5 presents a discussion of model results in the context of observed cyanobacterial blooms in Marion Reservoir; and, finally, conclusions and recommendations from this work are presented in Chapter 6.

Chapter 2 - Literature Review

HARMFUL CYANOBACTERIAL BLOOMS

Drinking water reservoirs in agricultural dominated watersheds are particularly vulnerable to Harmful Cyanobacterial Blooms (CyanoHABs). A byproduct of cyanobacteria is the production of objectionable taste and odor compounds that persist in drinking water supplies as well as a variety of toxins that can cause damage to the liver, kidneys and other organs if ingested. Cyanobacterial blooms pose severe ecological and economical threats in lakes and reservoirs. Ecological impacts include hypoxia and fish kills via cyanobacterial bloom contribution to eutrophication and depleting dissolved oxygen in the water column; blooms of cyanobacteria are not favorable for zooplankton, which could cause other food web disruptions [6] [7]. Economic impacts include loss of income to nearby communities for recreational uses, property value slumps, increased drinking water costs [8]. Understanding the complex physical transport and biological features of cyanobacteria is important for predicting blooms in freshwater systems [3].

Many things are known to play a part in causing HABs. Direct causes generally occur through nutrient inputs from the watershed and internal nutrient cycling. Agricultural, urban, and industrial nutrient sources have accelerated rapidly in the past several decades, overloading waterbodies with Nitrogen and Phosphorus [7]. Meteorological variables, including temperature and wind patterns are drivers as well. Temperature drives HABs largely by the warming climate around the world. Cyanobacteria that have adapted to hot conditions can easily outcompete the algae that’s growth decreases in warming climates [7]. Climate change will also increase vertical stratification due to warm surface waters. Consequently, as temperatures rise, lakes and reservoirs will stratify earlier in the warm season and stratification will last further into the fall [7].

Although the general drivers of CyanoHABs are understood, blooms remain site specific and difficult to predict as different water bodies respond differently to these variables. For example, a 2004 study looked at Clinton Lake (east central Kansas, USA) from May 1997 to September 1998 and spatial and temporal patterns of cyanobacteria abundance and composition were examined [9]. Specifically looking at the physical and chemical properties of Clinton Lake, the results indicated that nutrients, turbidity, and hydrologic regime were important pieces of creating and sustaining cyanobacterial blooms. Low levels of nitrogen along with internal release of phosphorus from the lake sediment under brief periods of anoxia possibly contribute as well [9].

A more involved study [10] presented a three-dimensional model for nonhydrostatic free surface flow and cyanobacteria transport and associated population dynamics is presented. The model was used to investigate transport and growth of cyanobacteria in another Kansas waterbody, Milford Lake. This study posed physical processes as being most effective to cyanobacteria distribution. This was specifically true with wind: when wind was low, water column turbidity had a greater effect on cyanobacteria distribution than temperature or ambient light [10].

Using satellite images and field samples from 2012 and 2013 at Lake Chaohu (Anhui Province, China), patterns of spatial and temporal shifts in cyanobacteria and their driving factors was studied [11]. The blooms primarily occupied the western region of the lake, and the direction and speed of the prevailing wind determined the spatial distribution of these blooms [11].

EFFECTS OF WIND ON BLOOMS

As suggested in the studies presented in the previous section, wind is one of many physical factors involved in both forming and sustaining CyanoHABs. Wind is particularly impactful to a waterbody's thermal structure. Along with wind, heating and cooling of lakes on the water's surface leads to thermal stratification and mixing over daily, seasonal, and annual periods. Stratification refers to the formation of distinct layers of different densities within the depth profile of a water body. Lakes and reservoirs generally have the following thermal structure: (1) an upper warmer mixed layer called the epilimnion; (2) a middle more stratified layer called the thermocline or metalimnion; and if deep enough (3) a bottom weakly stratified layer of colder and denser water called the hypolimnion [12]. Wind affects water column mixing by promoting either stratification with calm conditions versus well-mixed water bodies through stronger wind conditions. Stratification prevents vertical mixing of water, which in turn affects nutrient uptake by organism such as cyanobacteria. Nutrient and light availability during mixed versus stratified conditions may be associated with start and duration of blooms [12].

Several studies have explored the effects of wind on cyanobacterial blooms. For example, a 2016 study [13] separated winds influence into three components: (a) Direct Disturbance Impact (DDI) on cyan- bacterial proliferation, (b) Indirect Nutrient Impact (INI) by sediment release and (c) Direct Transportation Impact (DTI) by both gentle wind-induced surface drift and wave-generated Stokes drift. Each of the above's individual contributions to the May 2007 bloom event in Meiliang Bay, Lake Taihu (China) was investigated. Though location dependent, wind was found to promote the bloom 10.5%. Direct Transportation Impact had the strongest contribution of wind's impacts on blooms. Influencing weights of DTI, DDI and INI were 48.55%, 32.30% and 19.15% respectively [13].

A study [14] using long-term historical data and short-term field measurement helped to identify the importance of changes in wind patterns on the cyanobacterial blooms in Lake Taihu (China).The results of the research's regression analysis using multi-year satellite image data (via Floating Algae Index) concludes that the annual mean monthly maximum cyanobacterial bloom area (MMCBA) increased each year from 2000 to 2011. MMCBA was shown to be negatively correlated with wind speed. As Lake Taihu has become increasingly calm, changes in wind patterns related to this climate shift have promoted the increase of cyanobacterial blooms in the lake [14].

GENERAL LAKE MODEL

The diversity among lakes and reservoirs has led to many different modeling approaches and outcomes. This is a challenge within modeling, specifically hydrodynamic modeling. One-dimensional models using vertical profiles of temperature and density have found widespread use, especially for lakes and reservoirs, since they require minimal calibration and are highly efficient computationally [15].

One study [15] assessed how a one- dimensional lake model, the General Lake Model (GLM) performed with 32 lakes from a global observatory network (GLEON). Among the 32 water bodies was a range in size, climate, trophic level, etc. Several error assessment metrics were calculated to test the model. A sensitivity analysis was also completed for nine parameters relating to mixing efficiency. The results show that models input on an hourly scale perform better than those on a daily scale as expected, but outputs were generally less sensitive to uncertain inputs than expected [15].

A study [16] on Lake Maggiore (Northern Italy/Southern Switzerland) demonstrated that a calibrated enclosed-lake model can give satisfactory results only if it employs an unrealistically low light extinction coefficient, contradictory to expectation. This is hypothesized to be true in order to allow heating of the deep metalimnion and hypolimnion, whose real warming strongly depends on interflows that are ignored in this case. GLM was used to model the lake from 1998 to 2014 [16].

In summary: (1) there is evidence that wind influences timing and/or duration of cyanobacterial blooms, and (2) effects are lake specific. Understanding influence of wind in a lake or reservoir may help predict when blooms will develop and how cyanobacteria and/or their toxins may be distributed in the water column, which is particularly important in waterbodies used for recreation and/or water supply. In this thesis, effects of wind on mixing dynamics in Marion Reservoir and potential linkages to CyanoHABs are examined.

Chapter 3 - Methods

3.1 Study Site

Marion Reservoir is on the Cottonwood River northwest of Marion, KS, on the western edge of the Flint Hills region of Kansas, USA (see Figure 3.1). The reservoir is operated by the U.S. Army Corps of Engineers (USACE) and was completed in 1968. Though built mainly for flood control, the reservoir serves many purposes, including recreation like camping, fishing, and swimming. Marion Reservoir's conservation pool sits at elevation 411.6 m (1350.5 ft) and has a storage of 192 mm (7.56 inches of runoff or 80,658 acre-ft), based on a drainage area of 200 square miles.

Harmful cyanobacterial blooms have occurred at Marion since 2003 and are monitored by Kansas Department of Health and Environment's (KDHE) Harmful Algal Bloom Response program. Figure 3.2 shows the KDHE sampling sites at Marion Reservoir.

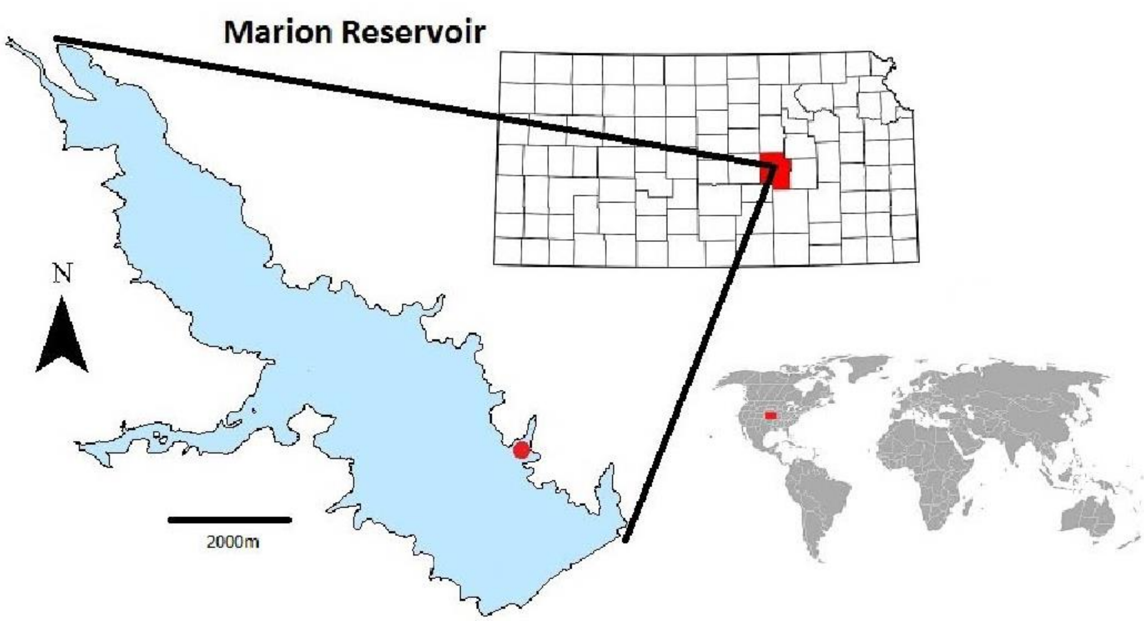

Figure 3.1 Location of Marion Reservoir within Kansas (image from [17]).

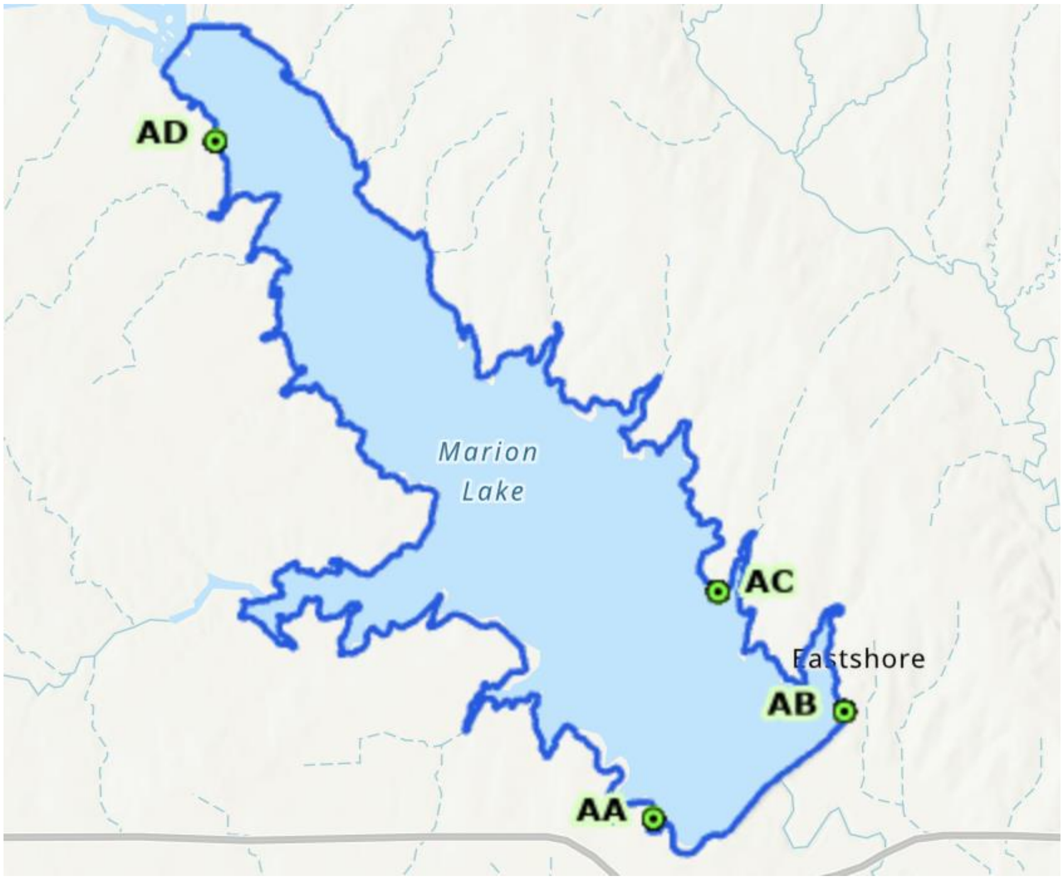

Figure 3.2 Map of Marion Reservoir with KDHE test sites (image from KDHE).

3.2 Numerical Model

The general lake model (GLM) was developed by the Aquatic EcoDynamics Research group at the University of Western Australia. The open-source, one-dimensional hydrodynamic model was designed to simulate the hydrodynamics of lakes, reservoirs, and wetlands. “The model is suitable for operation in a wide range of climate conditions and is able to simulate ice formation, as well as accommodating a range of atmospheric forcing conditions” [5]. The most recent version of GLM, version number 3.0, was used in this study. R was used as an interface for running GLM. Specifically, R code from computational limnologist Robert Ladwig via the GLEON 21.5 GLM workshop was adapted for the purposes of this research.

One-, two-, and three-dimensional models are each are capable of simulating seasonal changes in water temperature and stratification, however two- and three-dimensional models are able to consider additional variables such as flow velocities and lateral transport [18]. Though these higher dimensional models can consider more of the complexities of lakes and reservoirs and are useful in simulating transport dynamics, one-dimensional models are generally sufficient for modeling thermal stratification and mixing. As this was the primary goal of this research, along with not having the data necessary to calibrate two- or three-dimensional models, the limitations of the one-dimensional model were accepted.

As depicted in Figure 3.3, GLM resolves a vertical series of layers that capture the variation in water column properties in response to meteorological and hydrological (inflow and outflow) variables. Users may configure any number of inflows and outflows, and more advanced options exist for simulating aspects of the water and heat balance [5].

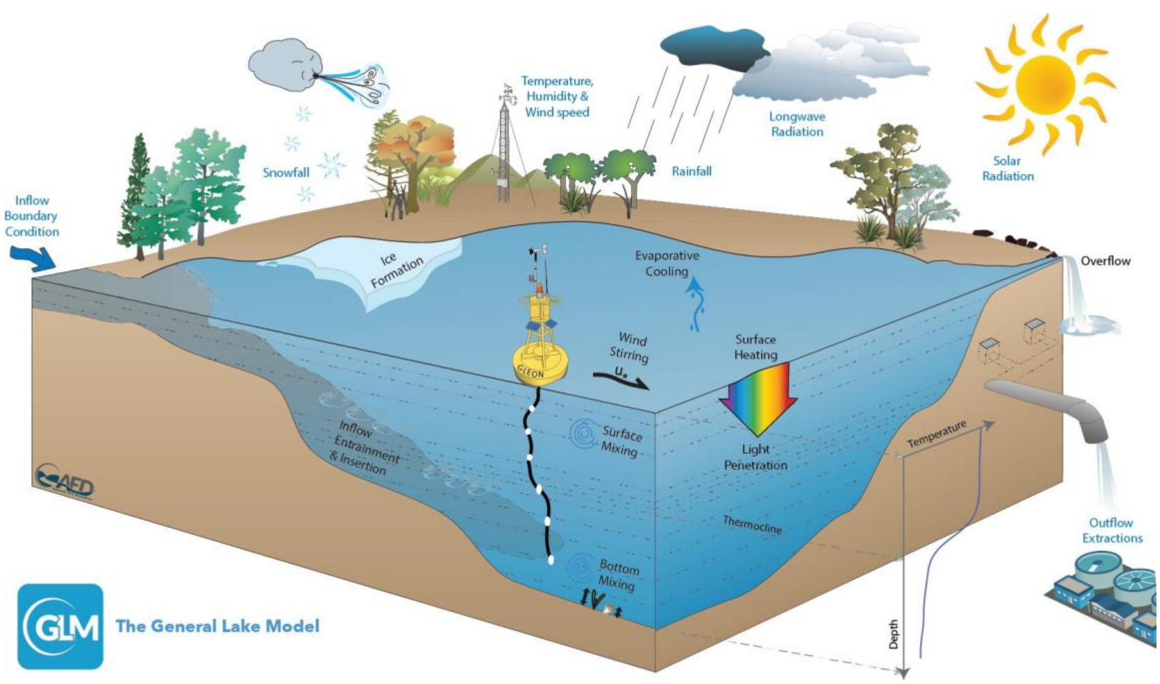

Figure 3.3 General Lake Model input and outputs flow chart (image from [5]).

3.3 Model Setup & Input Data

The model required time-series of meteorological variables, hydrological data on inflows and outflows as well as the morphometric information given as surface area at different water depth (hypsometric curve). Inflow and outflow data were provided on a daily time scale while hourly data were provided the meteorological timeseries data for the years 2022-2023. A summary of these required inputs and their sources is provided in Table 3.1.

Inflow and Outflow to Marion Reservoir were compiled on a daily timestep from the USACE. Likewise, Rainfall, Wind Speed, Relative Humidity, Shortwave Radiation, and Air Temperature were compiled on an hourly timestep from the USACE weather station located atop the dam at Marion Reservoir.

The GLM model requires longwave radiation fluxes as part of the surface energy balance. Longwave radiation was not directly measured as part of the USACE weather station; therefore, cloud cover was provided as an input such that longwave radiation could be calculated internally by GLM using a relationship between cloud cover fraction and longwave radiation proposed by Idso and Jackson [19]. Cloud cover data were not collected at the USACE weather station on the Marion Reservoir dam. Hourly cloud cover data were obtained instead from Visual Crossing for Marion, Kansas. Visual Crossing integrated historical data from nearby weather stations in Wichita and Newton, Kansas. Since hourly data were gathered from locations up to 95 km from Marion Reservoir, the sensitivity of the variable was examined in order to determine possible impacts of these cloud cover data. This was done by running simulations with increased (+50%, maximum value of 100% cloud cover) and decreased (-50%, minimum value of 0% cloud cover) cloud cover values across the entire timeframe.

GLM requires inputs of a stage-area relationship to define the morphometry of a water body. Recent bathymetric mapping of Marion Reservoir, completed in 2008 by the Kansas Biological Survey, was used to provide this information.

Table 3.1 GLM inputs sources and units.

Model Input [INPUT FILE]	2022 Data	2023 Data	Original source units	Model units
Inflow	USACE	USACE	cfs	m^3/s
Outflow	USACE	USACE	cfs	m^3/s
Rainfall [Rain]	USACE	USACE	in	m/day
Wind Speed [WindSpeed]	USACE	USACE	mph	m/s
Relative Humidity [RelHum]	USACE	USACE	%	%
Shortwave Radiation [ShortWave]	USACE	USACE	W/m^2	W/m^2
Air Temperature [AirTemp]	USACE	USACE	°F	°C
Cloudcover [Cloud]	Newton Airport	Visual Crossing	%	decimal
Temperature Profile	KSU	KSU	°C	°C
Bathymetry	KU Biological Survey	KU Biological Survey	ft	m

3.4 Model Calibration

Model parameters involved in the simulation of lake mixing dynamics can be calibrated using temperature profile data collected from the water body being simulated. Temperature profile data were collected using HOBO light and temperature loggers (Onset HOBO MX2201) which were suspended in Marion Reservoir near the dam. The loggers were positioned at depths of 0.1 m and 0.6 m below the water surface and then in 1-m increments to reservoir bottom (total depth of approximately 10.6 m; total of 12 loggers). Loggers were set to record in 1-hour increments.

Internal mixing parameters are physically or empirically derived and are intended to be transferable between different lakes [4]. GLM calibration was limited to a few lake-specific parameters based on inspection of model sensitivity (only sensitive parameters were selected for calibration) and recommended parameter calibration sets from the model developers and literature [4], [5]. Six parameters were initially considered for calibration: wind factor (f_U), vertical turbulent mixing coefficient in the hypolimnion (C_{HYP}), scaling factor to adjust the cloud data (f_{LW}), light attenuation coefficient (K_w), bulk aerodynamic transfer coefficient for sensible heat flux (C_H), and sediment mean temperature ($T_{z\ mean}$). A sensitivity analysis was done to determine which parameters were most sensitive using a sensitivity index, SI (Eq. 1).

The root-mean-square-error (RMSE) of water temperature was applied to assess model performance (Eq. 2), which is calculated as the sum of the squared differences in predicted and actual temperature *i* divided by the total number of observations *n*. The five parameters were then used to calibrate the model with 2022 data. While a longer calibration and validation period is desirable, temperature profile data against which to compare model predictions were only available for 2022 and 2023. Other studies using GLM have relied on a similar time period (1-2 years) for model calibration and verification [4]. To better visualize the model's fit at different depths in the profile, a linear regression between observed and simulated reservoir temperature at various depths was fit and the R-squared was calculated as an additional measure of model performance.

$$\mathrm{SI} = \frac{\frac{(\mathrm{Output_{new}} - \mathrm{Output_{original}})}{\mathrm{Output_{original}}}}{\frac{(\mathrm{Parameter_{new}} - \mathrm{Parameter_{original}})}{\mathrm{Parameter_{original}}}} \quad \text{(Eq. 1)}$$

Where:

$\mathrm{Output_{new}}$ = output with calibrated parameters
$\mathrm{Output_{original}}$ = output before calibration
$\mathrm{Parameter_{new}}$ = altered/calibrated input
$\mathrm{Parameter_{original}}$ = baseline input

$$\mathrm{RMSE} = \sqrt{\sum_{\mathrm{i}=1}^{\mathrm{n}} \frac{(\mathrm{Predicted_i} - \mathrm{Actual_i})^2}{n}} \quad \text{(Eq. 2)}$$

Where:

$\mathrm{Predicted_i}$ = modeled output
$\mathrm{Actual_i}$ = observed output
n = number of observations

3.5 Wind Scenarios

Previous analyses of wind temporal trends using both linear regression and Mann-Kendall trend analysis by Rahmani and Bhandari (unpublished) on historical (1973-2018) wind data from Newton, Kansas indicated a statistically significant decrease in the frequency of lower wind speeds (0.45 to 4.9 mph) and a corresponding increase in the frequency of higher wind speeds (8.5 to 8.9 mph). While the latter trend was not statistically significant, the decrease in low wind periods suggests that wind speeds experienced at Marion Reservoir may be increasing with time. In line with the goal of this thesis to examine effects of changing wind conditions on reservoir mixing in Marion Reservoir, two wind scenarios were developed to represent potential increases in wind speeds.

3.5.1 Scenario S1: Effect of uniform wind speed increases

After completing a baseline calibration on relevant wind parameters for 2022, observed wind magnitude was increased by 10% and 20% for the entirety of the 2022 and 2023 input meteorological dataset. This was done to determine the effect of a uniform wind speed increase on the stratification versus well-mixed conditions in Marion Reservoir. The 10% and 20% increases were selected based on observed variation in wind speed between the long-term average and the 25th to 75th percentiles about the mean.

3.5.2 Scenario S2: Sensitivity to wind speed under meteorological trends

Scenario S1 was developed to provide insight to the sensitivity of reservoir mixing to increasing wind speed; however, it is unlikely that future wind speeds would undergo a monotonic increase in both day and night across all seasons. Therefore, in an effort to show the future seasonal and daily variability in windspeed, a separate but complementary analysis to the analysis completed by Rahmani and Bhandari (not published) was completed. In this secondary analysis, available wind data from the airport station in Newton, Kansas (the nearest climate data station to Marion, located 26 miles to the southwest; data spanned 1992 to 2023) was divided into two equal periods (Period 1, 1992-2007 and Period 2, 2008-2023). Data during the growing season (May through September) was then extracted from each of these periods and divided into daylight and night periods. Then, the frequency of hourly wind observations was compared using the non-parametric Wilcoxon rank sum text between Period 1 and Period 2 as described by Saplioglu and Güçlü for both day and night periods within the following ranges of wind speed: <2.0 mph, 2.0-4.9 mph, 5.0-6.9 mph, 7.0-9.9 mph, 10.0-14.9 mph, 15.0-19.9 mph, and >20 mph [20].

The S2 scenario was intended to represent a more realistic pattern of wind speed change than the monotonic increases applied under S1 by taking seasonal and diurnal trends into account. This scenario was applied to the growing season only (May through August) of 2022 and 2023. As with S1, sensitivity to applied wind speed changes was evaluated using the Lake Number and comparing baseline conditions to altered conditions.

3.6 Evaluation of Simulations & Relating to Bloom Timing

An indicator of wind-driven mixing known as the Lake Number (LN) was used to relate GLM results to field observations of cyanobacterial blooms in Marion. The LN is a dimensionless parameter [21] and quantitative indicator of the potential for wind-driven mixing across the thermocline. The GLM model computes the Lake Number on a daily time step according to Equations 3 and 4.

$$L_N = \frac{g \text{ x } S_t \text{ x } \left(1 - \frac{Z_t}{Z_m}\right)}{p_m \text{ x } u_*^2 \text{ x } A_m^{1.5} \text{ x } \left(1 - \frac{Z_g}{Z_m}\right)} \quad \text{(Eq. 3)}$$

Where:

g = acceleration of gravity (980 cm s^{-2})
S_t = Schmidt Stability [g cm cm^{-2}]
Z_t = thermocline height [cm] above the bottom
Z_m = maximum depth of the lake [cm]
p_m = water density at surface [g cm^{-3}]
u_*^2 = water friction velocity [cm s^{-1}] due to wind stress (approximated by the bulk aerodynamic formula in Eq. 4 below)
A_m = surface area of the lake [cm^2]
Z_g = center of volume in [cm] above the bottom

$$u_*^2 = \frac{p_a}{p_m} \text{ x } C_D \text{ x } U_{10}^2 \quad \text{(Eq. 4)}$$

Where:

U_{10} = wind velocity at 10 m above water surface [cm s^{-1}]
C_D = Drag Coefficient = 1.3 x 10^{-3} [dimensionless]
$\frac{p_a}{p_m}$ = ratio between air and water densities = 1.2 x 10^{-3} [dimensionless]

The LN can be interpreted as follows: large values of LN indicate that thermal and/or salinity-driven stratification is strong and persists despite forces introduced by surface wind stress. In these cases, one would expect minimal mixing below the thermocline (e.g., in the metalimnion or epilimnion) and therefore minimal exchange of nutrients released at the sediment-water interface. A LN equal to one indicates a threshold in which the wind is just sufficient to lift the thermocline to the water surface at the most upwind point in the lake such that the lake is about to tip to experience some degree of wind-mixing. For very small values of LN, stratification is expected to be very weak relative to wind forces at the water surface such that turbulent mixing is expected throughout the water profile. Under these conditions, exchange of nutrients and other materials between the surface/photic zone and lower epi- and hypolimnion are likely.

The timing and duration of cyanobacterial blooms in Marion were obtained from field observations documented by the Kansas Department of Health and Environment's (KDHE) Harmful Algal Bloom Response program, which documents confirmed blooms in public waterbodies across the state, including Marion Reservoir. Modeled lake numbers and associated patterns of mixing and stratification within the water column were then compared to the dates at which blooms were detected to explore potential relationships between bloom onset and persistence with reservoir mixing status.

Chapter 4 - Results & Discussion

4.1 GLM Calibration Results

All parameters except sediment mean temperature were determined to be sensitive enough, that is SI greater than 0.1, for calibration [4]. Table 4.1 presents the final set of calibrated parameter values that were further validated against 2023 temperature profile data. The RMSE for the 2022 calibration period was 1.11 °C while the RMSE for the 2023 validation periods was 1.45 °C. A comparison of observed and simulated lake temperature profile data following model calibration is shown in Figure 4.1.

RMSE was used to evaluate calibration results, where a lower RMSE indicated a better fit by the model. As an absolute measure of fit, RMSE gives an idea of the average difference between the observed data values and the predicted data values. R-squared can give a better understanding of the acceptability of the fit visually and potential bias such as over versus under prediction or differing performance for higher versus lower temperatures. R-squared was computed for the linear regression between observed and modeled temperature data at depths of 1-m, 5-m, and 8-m for 2022. R-squared at all three depths was 0.9669, and the plot can be seen in Figure 4.2 (plots for each individual depth can be found in Appendix). The results of the R-squared analysis show model performance is well fit and does not systematically over or under predict temperature.

Table 4.1 Calibrated GLM parameters: wind factor, vertical turbulent mixing coefficient in the hypolimnion, scaling factor to adjust the cloud data (lw), light attenuation coefficient (Kw), and bulk aerodynamic transfer coefficient for sensible heat flux (ch).

Parameter	Original Value	Calibrated Value	[Lower Bound, Upper Bound]
wind_factor	1.00	1.40	[0.7,2]
coef_mix_hyp	0.50	0.53	[0.4,0.6]
lw_factor	1.00	1.41	[0.7,2]
Kw	0.80	0.10	[0.1,0.8]
ch	0.0013	0.0018	[0.0005,0.002]

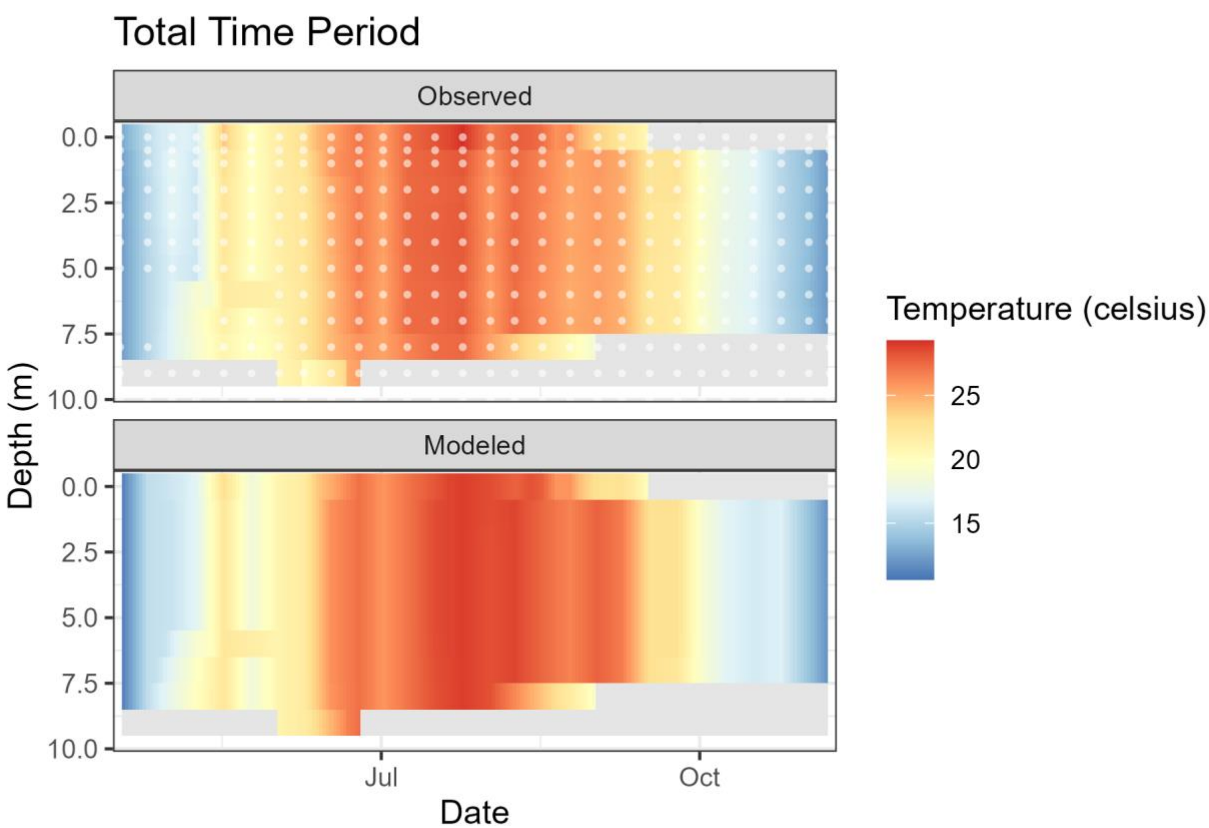

Figure 4.1 Observed vs. Modeled temperature profile for Marion Reservoir in 2022.

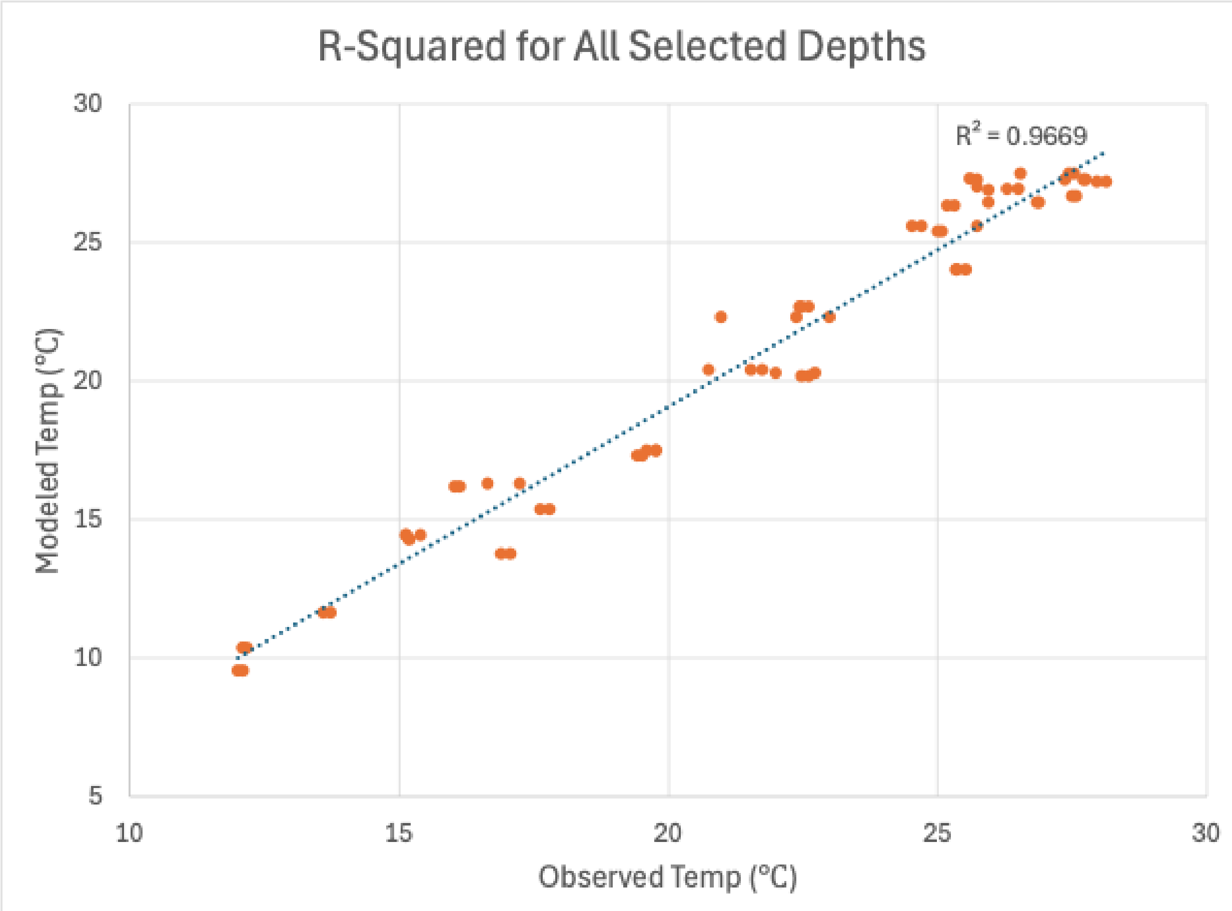

Figure 4.2 Observed vs modeled temperature at 1-m, 5-m, and 8-m depths with R-squared.

4.2 Marion Reservoir Mixing Status from 2022 to 2023

This study uses 2022-2023 meteorological data for Marion Reservoir. 2022 was a near average year with respect to precipitation and wind conditions, and 2023 was a dry, relatively still year, as shown in Table 4.2. Figure 4.3 presents a modeled Lake Numbers (LN) for both years as an indicated of wind-driven mechanical mixing. Comparing the two years, baseline conditions indicate both have weak stratification with respect to wind stress as indicated by the high frequency of LN values less than 1. The median LN in 2022 was 8.25×10^{-5} while the median in 2023 was 9.33×10^{-4}. Thus, while both years exhibited frequent mixing, LN values were lower overall in 2022, indicating 2022 was more mixed and 2023 was less mixed.

Frequency distribution of LN values output each day for the given year (Jan-Dec) are shown in the following figures in this chapter. The y-axis indicates the percent of the dataset that has a value that is less than the value at that percentage. The data are presented in this way to illustrate shifts in the annual and seasonal distributions of LN number and consequently mixing status.

Table 4.2 Meteorological comparison between 2022 and 2023 (collected and compiled by USACE at Marion Reservoir) and historical (2000-2020) data (collected at Newton Airport and compiled by Iowa State University Mesonet).

	2022	2023	Historical
May			
Average air temperature (°C) [°F]	19 [66]	20 [67]	18 [65]
Average wind speed (m/s) [mph]	4.9 [11.0]	3.8 [8.5]	5.1 [11.3]
Total precipitation (mm) [in]	144 [5.67]	30 [1.19]	122 [4.78]
June			
Average air temperature (°C) [°F]	25 [77]	24 [75]	24 [76]
Average wind speed (m/s) [mph]	4.2 [9.4]	3.1 [7.0]	5.2 [11.7]
Total precipitation (mm) [in]	121 [4.78]	57 [2.24]	111 [4.36]
July			
Average air temperature (°C) [°F]	27 [81]	26 [80]	27 [80]
Average wind speed (m/s) [mph]	3.6 [8.0]	3.4 [7.7]	4.5 [10.0]
Total precipitation (mm) [in]	81 [3.19]	55 [2.17]	94 [3.72]
August			
Average air temperature (°C) [°F]	26 [80]	27 [81]	26 [78]
Average wind speed (m/s) [mph]	3.1 [7.0]	3.6 [8.0]	4.2 [9.4]
Total precipitation (mm) [in]	45 [1.77]	31 [1.24]	89 [3.52]

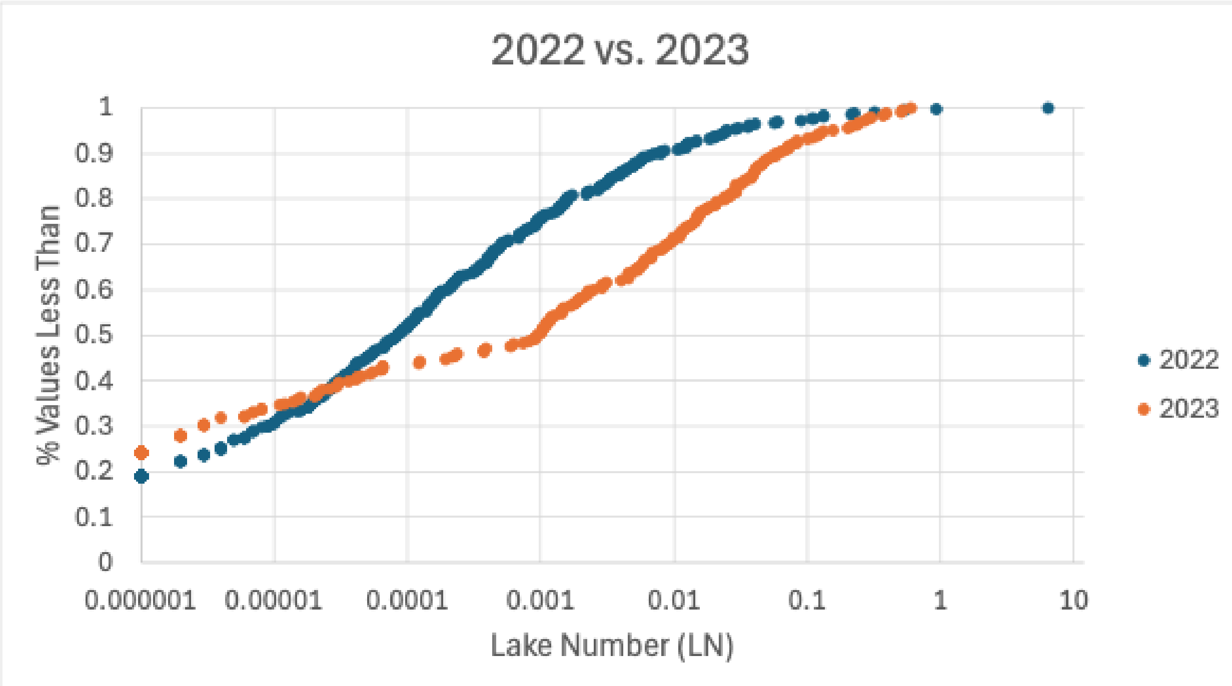

Figure 4.3 2022 vs. 2023 Lake Number (LN) value occurrence.

4.3 Scenario S1 Results

The influence of uniform increases in wind speed on water column stability in Marion Reservoir was evaluated using the Lake Number after applying a 10% and 20% increase in observed 2022 and 2023 wind speed data input to the GLM model.

The effect of these different wind speeds on the stratification in Marion Reservoir in 2022 and 2023 can be seen in Figures 4.4 and 4.5 respectively. In both years, the increases in wind magnitude created a corresponding decrease in Lake Number. The median LN value in 2022 shifted from 8.25 x 10^{-5} to 4.90 x 10^{-5} (41% decrease) under the 10% increase and to 3.9 x 10^{-5} (53% decrease) under the 20% increase in wind speed. Likewise, the median LN value in 2023 shifted from 9.33 x 10^{-4} to 5.08 x 10^{-4} (46% decrease) under the 10% increase and to 2.66 x 10^{-4} (71% decrease) under the 20% increase in wind speed. A 10% and 20% increase resulted in a nonlinear shift in median value. The resultant shift was far greater than 10% or 20%. This was expected, as stronger winds are generally indicative of weaker stratification and stronger mixing.

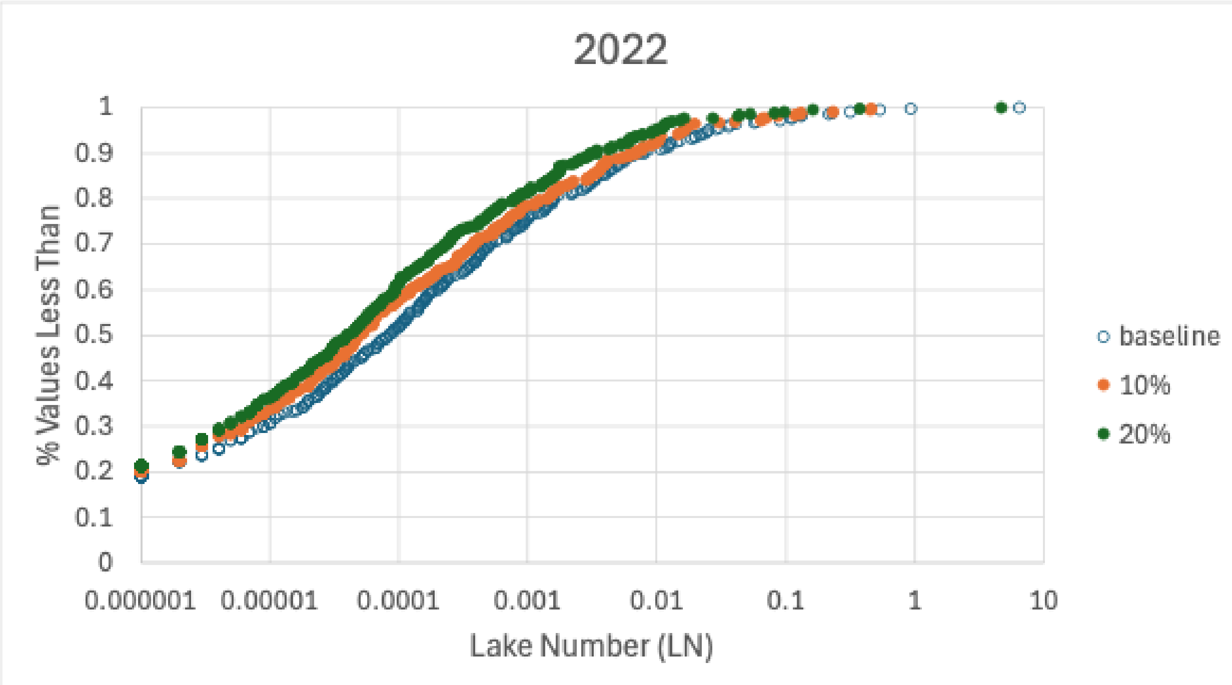

Figure 4.4 2022 with S1 scenario LN value occurrence.

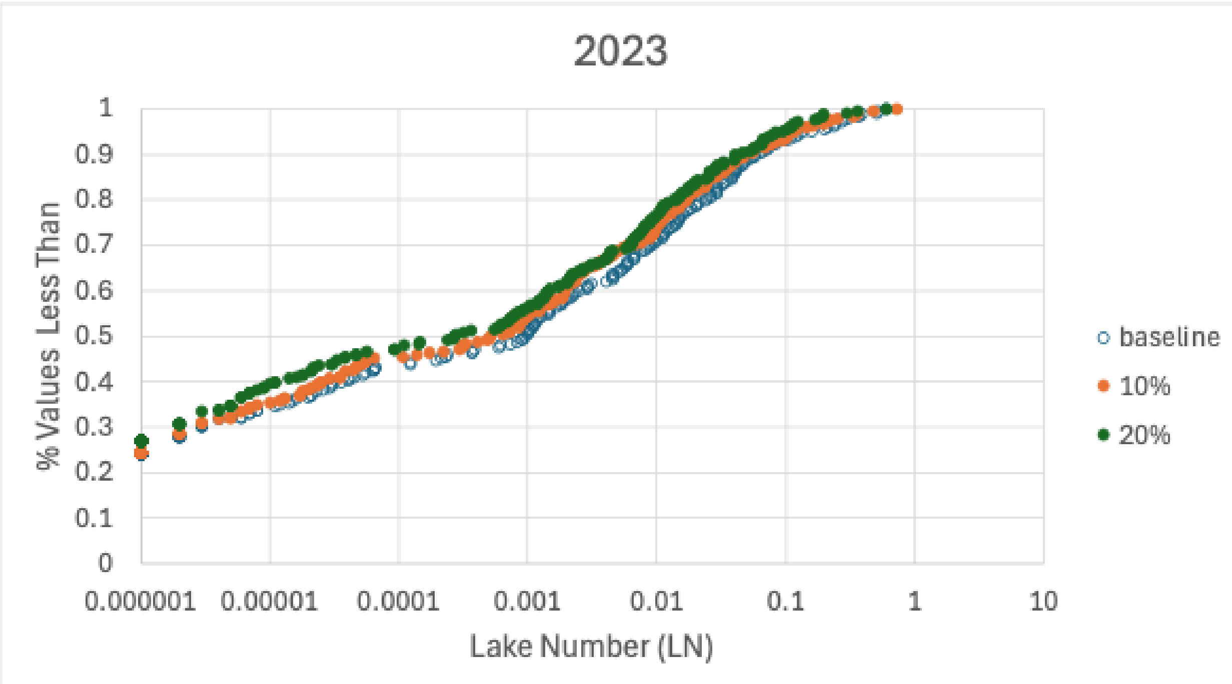

Figure 4.5 2023 with S1 scenario LN value occurrence.

4.4 Scenario S2 Results

Like the trend analysis by Rahmani and Bhandari, this analysis indicated a general increase in the frequency of high wind periods and a corresponding decrease in the frequency of low wind periods over time (i.e., between Periods 1 and 2). Consideration of both daylight and night periods in this analysis detected statistically significant ($p<0.05$) decreases in the frequency of low winds with corresponding, statistically significant ($p<0.05$) increases in higher winds during nighttime periods in May through August. Average daily temperatures are highest in these four months, and the vast majority of blooms in past years have occurred within these months. Since bloom conditions become favorable in May and begin to become unfavorable after August, this timeframe was selected. Comparisons of daytime wind speeds were more variable, with significant decreases in the frequency of lower wind speeds (< 7 mph) and increases in higher wind speeds (> 15 mph) detected in May and June, while July and August generally exhibited the opposite pattern with an increasing frequency of low winds and decreasing frequency of higher winds. These general patterns were represented in a second wind scenario, S2. In this scenario, hourly windspeed observations from May-June in 2022 and 2023 were adjusted to match the shift in wind frequencies such that there was a decrease in wind speeds ranging from 2 to 7 mph and an increase in wind speeds greater than 15 mph. In July and August, observed wind speeds were adjusted to match the increased frequency of lower winds (5 to 7 mph) and decrease in the frequency of wind speeds exceeding 15 mph.

The results of these changes for 2022 and 2023 can be seen in Figures 4.6 and 4.7 for the May through August time period to which the S2 scenario was applied. For 2022, the changes resulted in no change in the median LN value (0.0001). However, LN values below this median value tended to be higher under the S2 scenario, while LN values above this median value tended to be lower. The shift in LN is most notable at values approaching stratification (LN 0.1 to 1) with nearly an order of magnitude difference, which indicates overall stronger mixing under the S2 scenario. For 2023, however, LN predicted for the S2 scenario resulted in almost no change from baseline conditions.

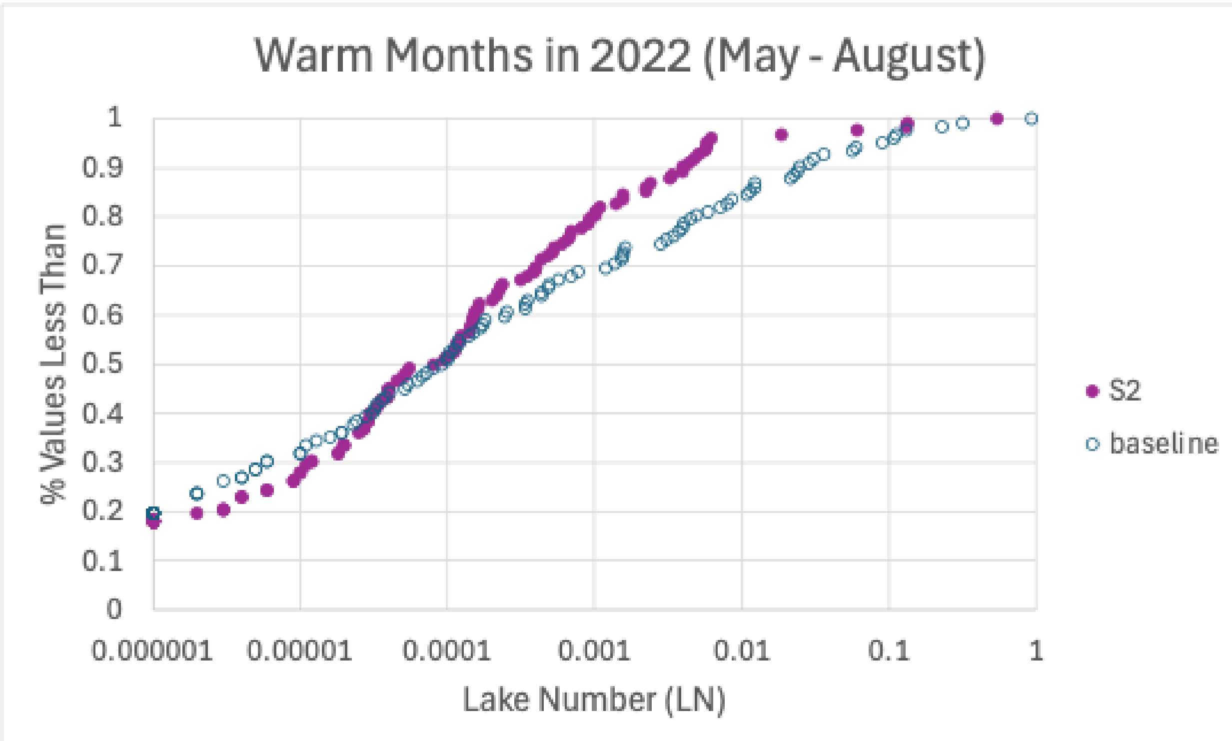

Figure 4.6 Warm months corresponding to typical cyanobacterial bloom season in 2022 LN value occurrence.

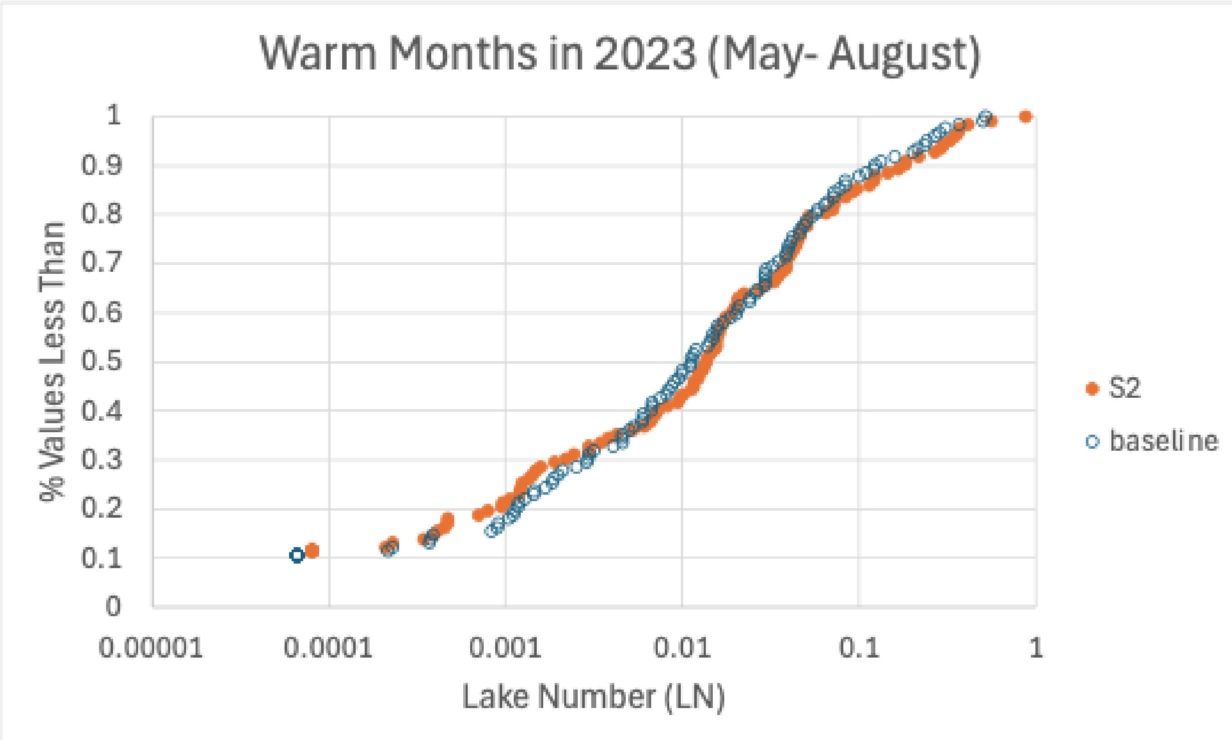

Figure 4.7 Warm months corresponding to typical cyanobacterial bloom season in 2023 LN value occurrence.

Chapter 5 - Discussion

Trend analyses of historic wind data collected near Marion Reservoir indicates reduced frequency of low wind periods and increased frequency of high wind periods, particularly during late spring and early summer. Higher and longer periods of strong mixing in Marion could be expected to cause the following: more even distribution of temperature, nutrients, and phytoplankton (including cyanobacteria) throughout the entirety of the water column. This condition may prevent the appearance of blooms by keeping cyanobacteria distributed throughout the water column (as opposed to concentrated in the surface waters). It may also allow access to nutrients released from the sediment if anoxic conditions develop.

The one-dimensional General Lake Model (GLM) was developed for Marion Reservoir to further examine the effects of wind speed on reservoir mixing and to make connections with observed CyanoHABs. To accomplish this objective, the S1 and S2 scenarios were applied to the calibrated GLM model. As expected, the uniform increases in wind speed applied in S1 resulted in a corresponding decrease in LN, which indicates stronger mixing. The S2 scenario, which reflected potential monthly trends in wind speed during the peak growing period for cyanobacteria (May to August) also indicated a shift to greater mixing when applied to 2022 data but not to 2023. The lack of response to the S2 scenario as applied to the 2023 meteorological record may have been due to the lower-than-average observed wind speeds to which the shifts in wind speed under S2 were applied. In other words, the wind peaks and lows in the 2023 S2 scenario may not have reached a large (or low) enough magnitude to elicit a substantial change in modeled temperature and mixing regimes.

The third objective of this thesis was to examine mixing status as indicated by the Lake Number and its relation to cyanobacterial bloom timing win Marion Reservoir. To help answer this question, or at least shed some light on it, LN was plotted against recorded bloom events at Marion Reservoir. In Figures 5.1 and 5.2, the week leading up to each KDHE tested and confirmed bloom event is highlighted. The 7-day period leading up to the confirmed bloom report is highlighted to account for the lag between the time that the bloom actually occurs, when it is reported to KDHE, and then when KDHE completes its sampling and analysis verification process to confirm the presence of a bloom. It is difficult to determine a pattern among the corresponding Lake Number due to its variability and steady blooms, specifically in 2022. In 2023, it is a bit easier to see trends in LN. For both years, there seems to be a pattern of rapid increase in LN (indicating increasing water column stability) following a low point (at which point the water column would be well mixed). This would make sense as strong winds after relative stillness can trigger new nutrient uptake.

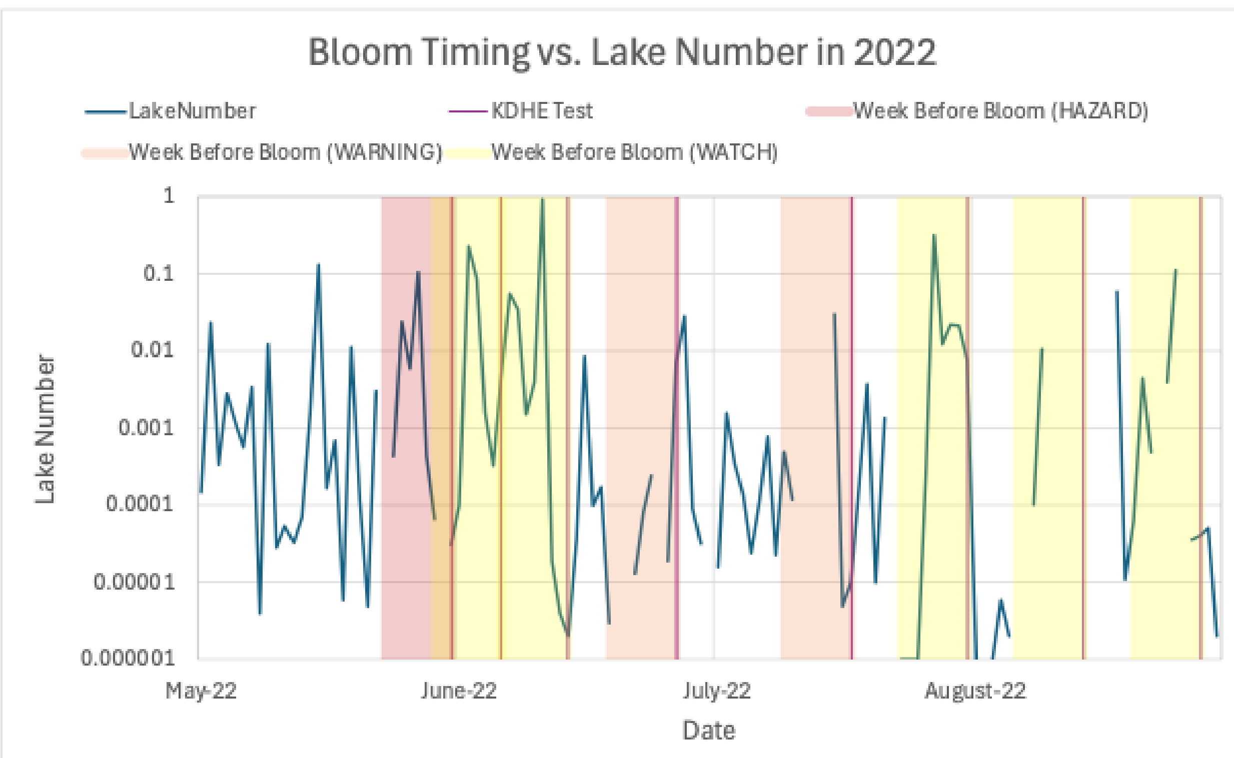

Figure 5.1 Bloom Timing vs Lake Number in 2022 (breaks in graph indicate a zero LN).

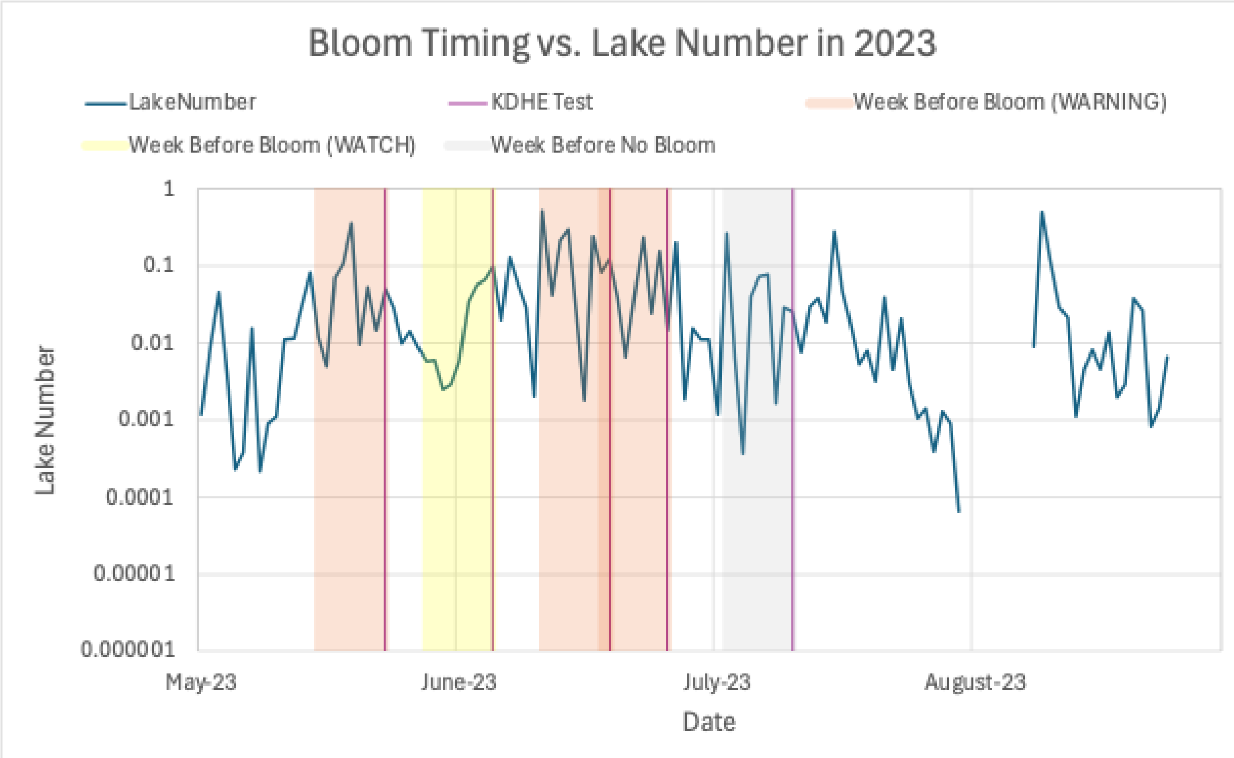

Figure 5.2 Bloom Timing vs Lake Number in 2023 (breaks in graph indicate a zero LN).

Results from similar studies suggest similar impacts by wind, though there are no similarly located studies where comparisons can be made due to model methodology being different. Other shallow eutrophic lakes have exhibited comparable behavior. The earlier mentioned study conducted in Germany had similar results indicating the clear impact wind speed has on stratification. Though the reservoir studied in Germany experienced similar wind conditions, the reservoir itself is significantly larger and the climate there was colder [4].

There are many limitations to consider with this research. First, model limitations inherent to the methods used limit the study to a simplistic nature. Second, limitations in analysis due to datasets and locations. All major limitations are discussed below.

- The nature of 1-D modeling included many limitations in order to keep computations simple. Specifically for modeling such as with GLM, elements like flow direction and distribution are assumed as a constant rather than computed.

- Limited data availability also limited model creation and the conclusions that can be drawn. Since temperature profile data were only available for the years 2022 and 2023, calibration reference period is greatly limited, leading to the year 2022 being used as a reference year despite any differences among subsequent years, as discussed further below.
- Comparing the HABs of 2023 using calibrated 2022 variables is particularly challenging due to 2022 exhibiting more intense bloom events across the warm season - potentially due to 2022 having higher than average water levels. The lack of data for more years to calibrate against mentioned above contributes to this limitation.
- HABs are monitored and tested along the shores of Marion Reservoir, and temperature profile data was collected close to the dam. However, the model represents lake conditions at a more central location within the reservoir. This difference could potentially contribute to variance in temperature data.
- As stated, cloud cover hourly data was gathered from a separate location. The sensitivity of the variable was examined to determine possible limitations of using the dataset. This was done by running simulations with increased and decreased cloud cover values and examining impacts on LN values. Results of this sensitivity test are shown below in Table 4.3. As below, baseline conditions and altered conditions had little variance and therefore it can be concluded that cloud cover differences from using the separate location data is likely negligible in LN contributions.

Table 5.1 Cloud cover sensitivity on LN analysis results.

	Baseline	50% Increase	50% Decrease
Average	0.34	0.34	0.36
Standard Deviation	5.89	5.89	6.35
Maximum	112.18	112.21	120.94
Minimum	0.00	0.00	0.00

Chapter 6 - Conclusions

With concerns of CyanoHABs in freshwater aquatic systems, including reservoirs throughout Kansas, the impact of wind events on the stratification dynamics within reservoirs and consequent HAB conditions is of great importance.

This research study used the General Lake Model (GLM) to analyze the effects of different wind scenarios on stratification and potential for harmful cyanobacterial blooms in Marion Reservoir. The GLM model was calibrated and verified using temperature profile data collected from Marion Reservoir in 2022 and 2023. Wind scenarios reflecting potential changes in wind speed during the algal bloom season were then applied in the model to examine the effects of wind on reservoir mixing dynamics. The relationship between modeled mixing indicators and documented blooms was explored, but this research illustrates the crucial impact of wind magnitude on stratification of lakes and reservoirs and further research into resulting HABs.

References

[1] L. González-Madina et al., “Drivers of cyanobacteria dominance, composition and nitrogen fixing behavior in a shallow lake with alternative regimes in time and space, Laguna del Sauce (Maldonado, Uruguay),” *Hydrobiologica*, vol. 829, pp. 61-76, 2019.

[2] S. Krishna et al., “Model-based data analysis of the effect of winter mixing on primary production in a lake under reoligotrophication,” *Ecological Modelling*, vol. 440, 2021.

[3] H. Paerl and J. Huisman, “Blooms Like It Hot,” *SCIENCE*, vol. 320, pp. 57-58, 2008.

[4] C. Mi, M. Frassl, B. Boehrer, and K. Rinke, “Episodic wind events induce persistent shifts in the thermal stratification of a reservoir (Rappbode Reservoir, Germany),” *International Review of Hydrobiology*, vol. 103, pp. 71-82, 2018.

[5] M. Hipsey et al., “A General Lake Model (GLM 3.0) for linking with high-frequency sensor data from the Global Lake Ecological Observatory Network (GLEON),” *Geoscientific Model Development*, vol. 12, pp. 473-523, 2019.

[6] A. Sukenik, A. Quesada, and N. Salmaso, “Global expansion of toxic and non-toxic cyanobacteria: effect on ecosystem functioning,” *Biodiversity and Conservation*, vol. 24, pp. 889-908, 2015.

[7] H. Paerl and T. Otten, “Harmful Cyanobacterial Blooms: Causes, Consequences, and Controls,” *Microbial Ecology*, vol. 65, pp. 995-1010, 2013.

[8] J. Zhang, D. Phaneuf, and B. Schaeffer, “Property values and cyanobacterial algal blooms: Evidence from satellite monitoring of Inland Lakes,” *Ecological Economics*, vol. 199, 2022.

[9] S. Wang et al., “Relationships between cyanobacterial production and the physical and chemical properties of a Midwestern Reservoir, USA,” *Hydrobiologica*, vol. 541, pp. 29-43, 2005.

[10] H. Liu, Z. Zhenga, B. Youngb, and T. Harris, “Three-dimensional numerical modeling of the cyanobacterium Microcystis transport and its population dynamics in a large freshwater reservoir,” *Ecological Modelling*, vol. 398, pp. 20-34, 2019.

[11] M. Zhang et al., “Spatial and seasonal shifts in bloom-forming cyanobacteria in Lake Chaohu: Patterns and driving factors,” *Phycological Research*, vol. 64, pp. 44-55, 2016.

[12] S. MacIntyre and D. Hamilton, “Fate of Heat,” in Wetzel’s Limnology, I. Jones and J. Smol, Eds., London, UK: Academic Press, 2023, pp. 95-153.

[13] H. Wang et al., “Separation of wind's influence on harmful cyanobacterial blooms,” *Water Research: A Journal of the International Water Association*, vol. 98, pp. 280-292, 2016.

[14] T. Wu et al., “The influence of changes in wind patterns on the areal extension of surface cyanobacterial blooms in a large shallow lake in China,” *Science of the Total Environment*, vol. 518-519, pp. 24-30, 2015.

[15] L. Bruce et al., “A multi-lake comparative analysis of the General Lake Model (GLM): Stress-testing across a global observatory network,” *Environmental Modelling & Software*, vol. 102, pp. 274-291, 2018.

[16] A. Fenocchi, M. Rogora, S. Sibillaa, and C. Dresti, “Relevance of inflows on the thermodynamic structure and on the modeling of a deep subalpine lake (Lake Maggiore, Northern Italy/Southern Switzerland),” *Limnologica*, vol. 63, pp. 42-56, 2017.

[17] S. Delmott and D. Edds, “Zebra mussel maturation and seasonal gametogenesis in Marion Reservoir, Kansas, USA,” *BioInvasions Records*, vol. 3, pp. 247-260, 2014.

[18] M. Ishikawa et al., “Effects of dimensionality on the performance of hydrodynamic models for stratified lakes and reservoirs,” *Geoscientific Model Development*, vol. 15, pp. 2197-2220, 2022.

[19] S. Idso and R. Jackson, “Thermal radiation from the atmosphere,” *Journal of Geophysical Research*, 1969, https://doi.org/10.1029/JC074i023p05397.

[20] K. Saplioglu and Y.S. Güçlü, “Combination of Wilcoxon test and scatter diagram for trend analysis of hydrological data,” *Journal of Hydrology*, vol. 612, 2022.

[21] D. Robertson and J. Imberger, “Lake Number, a Quantitative Indicator of Mixing Used to Estimate Changes in Dissolved Oxygen,” *Int. Revue ges. Hydrobiol.*, vol. 79, pp. 159-176, 1994.

Appendix A - GLM input file & model performance

```
&glm_setup
   sim_name = 'Marion'
   max_layers = 75
   min_layer_vol = 0.1
   min_layer_thick = 0.15
   max_layer_thick = 1.5
   density_model = 1
/
&wq_setup
   wq_lib = 'aed2'
   wq_nml_file = 'aed2/aed2.nml'
   ode_method = 1
   split_factor = 1
   bioshade_feedback = .true.
   repair_state = .true.
   mobility_off = .false.
/
&light
   light_mode = 0
   n_bands = 4
   light_extc = 1, 0.5, 2, 4
   energy_frac = 0.51, 0.45, 0.035, 0.005
   Benthic_Imin = 10
   Kw = 0.1
/
&mixing
   surface_mixing = 1
   coef_mix_conv = 0.125
   coef_wind_stir = 0.23
   coef_mix_shear = 0.2
   coef_mix_turb = 0.51
   coef_mix_KH = 0.3
   coef_mix_hyp = 0.53
   deep_mixing = 2
   diff = 0
/
&morphometry
   lake_name = 'MarionReservoir'
   latitude = 38.4
   longitude = -97.12
   crest_elev = 414.5
   bsn_len = 11426
   bsn_wid = 2735
   bsn_vals = 31
   H = 402.03, 402.34, 402.64, 402.95, 403.25,
403.56, 403.86, 404.16, 404.47, 404.77, 405.08,
405.38, 405.69, 405.99, 406.3, 406.6, 406.91,
407.21, 407.52, 407.82, 408.13, 408.43, 408.74,
409.04, 409.35, 409.65, 409.96, 410.26, 410.57,
410.87, 411.18
   A = 4047, 89031, 190202, 315655, 501810,
793184, 1299041, 1999147, 2808518, 3694780,
4516292, 5333757, 6260487, 6940359, 7616184,
8433649, 9255161, 10157610, 11161230, 12294350,
13443657, 14694136, 15766553, 16810642, 17789981,
18777414, 19813409, 20926295, 22144398, 23435346,
24297326
/
&time
   timefmt = 2
   start = '2022-01-01 00:00:00'
   stop = '2022-12-31 00:00:00'
   dt = 3600
   num_days = 364
   timezone = -6
/
&output
   out_dir = 'output'
   out_fn = 'output'
   nsave = 6
   csv_lake_fname = 'lake'
   csv_point_nlevs = 4
   csv_point_fname = 'WQ_'
   csv_point_at = 1, 5, 8, 10
   csv_point_nvars = 2
   csv_point_vars = 'temp','salt'
   csv_outlet_allinone = .false.
   csv_outlet_fname = 'outlet_'
   csv_outlet_nvars = 3
   csv_outlet_vars = 'flow','temp','salt'
   csv_ovrflw_fname = 'overflow'
/
&init_profiles
   lake_depth = 8.7
   num_depths = 2
   the_depths = 1, 8.5
   the_temps = 0, 1
   the_sals = 0.4, 0.4
   num_wq_vars = 2
   wq_names = 'OXY_oxy','TRC_s1'
   wq_init_vals = 200.1, 200.2, 6.2, 6.2
/
&meteorology
   met_sw = .true.
   lw_type = 'LW_CC'
   rain_sw = .false.
   atm_stab = .false.
   catchrain = .true.
   rad_mode = 1
   albedo_mode = 1
   cloud_mode = 1
   meteo_fl = 'bcs/meteo.csv'
   subdaily = .true.
   wind_factor = 1.40
   sw_factor = 1.4
   lw_factor = 1.41
   at_factor = 1
   rh_factor = 1
   rain_factor = 1
   cd = 0.0013
   ce = 0.0013
   ch = 0.0018
   rain_threshold = 0.001
   runoff_coef = 0
   time_fmt = 'YYYY-MM-DD hh:mm:ss'
/
&inflow
   num_inflows = 1
   names_of_strms = 'Cottonwood'
   subm_flag = .false., .false.
   strm_hf_angle = 65
   strmbd_slope = 1
   strmbd_drag = 0.016
   inflow_factor = 1
   inflow_fl = 'bcs/cottonwood.csv'
   inflow_varnum = 3
   inflow_vars = 'FLOW','TEMP','SALT'
   coef_inf_entrain = 0
/
```

Appendix A Figure A.1 2022 example .nml file for GLM.

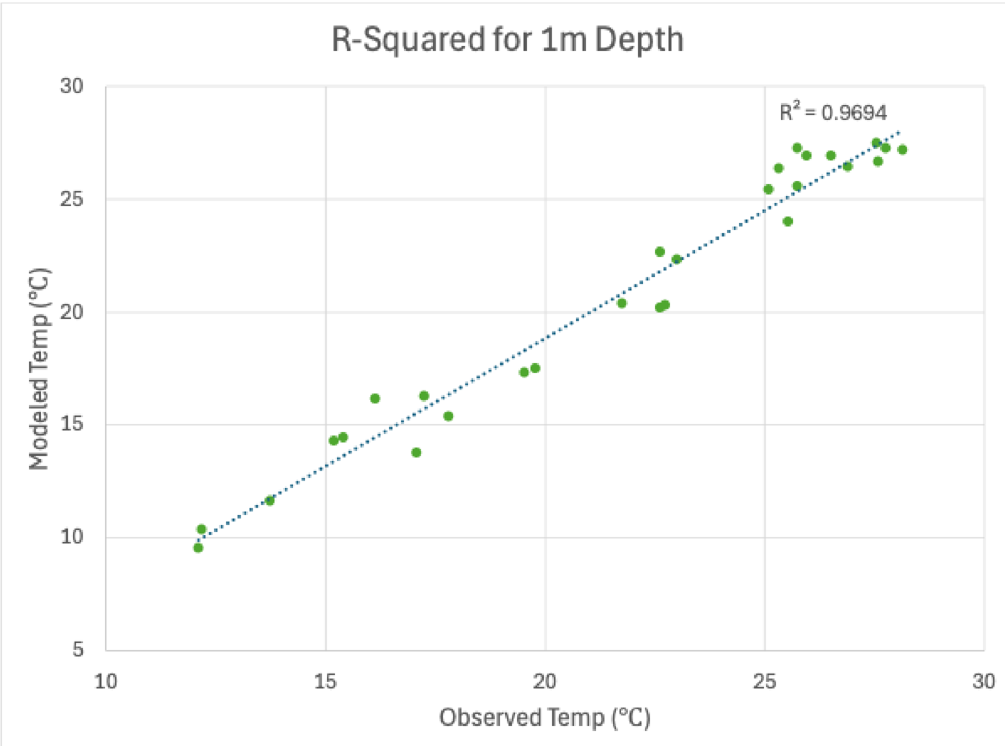

Appendix A Figure A.2 Observed vs modeled temperature at 1-m with R-squared.

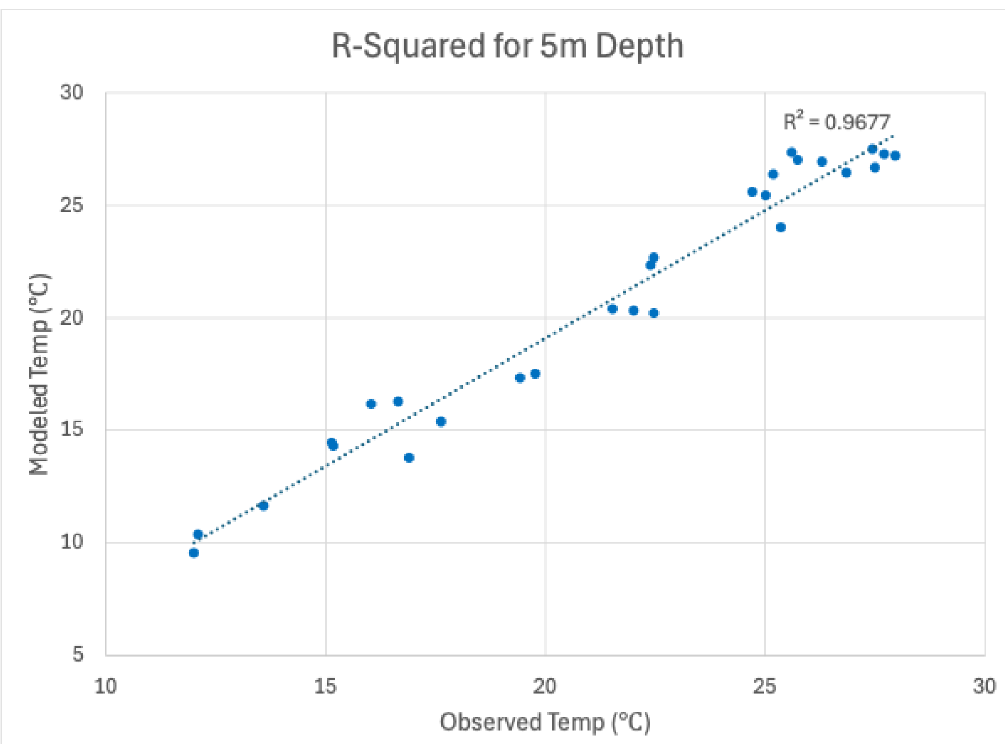

Appendix A Figure A.3 Observed vs modeled temperature at 5-m with R-squared.

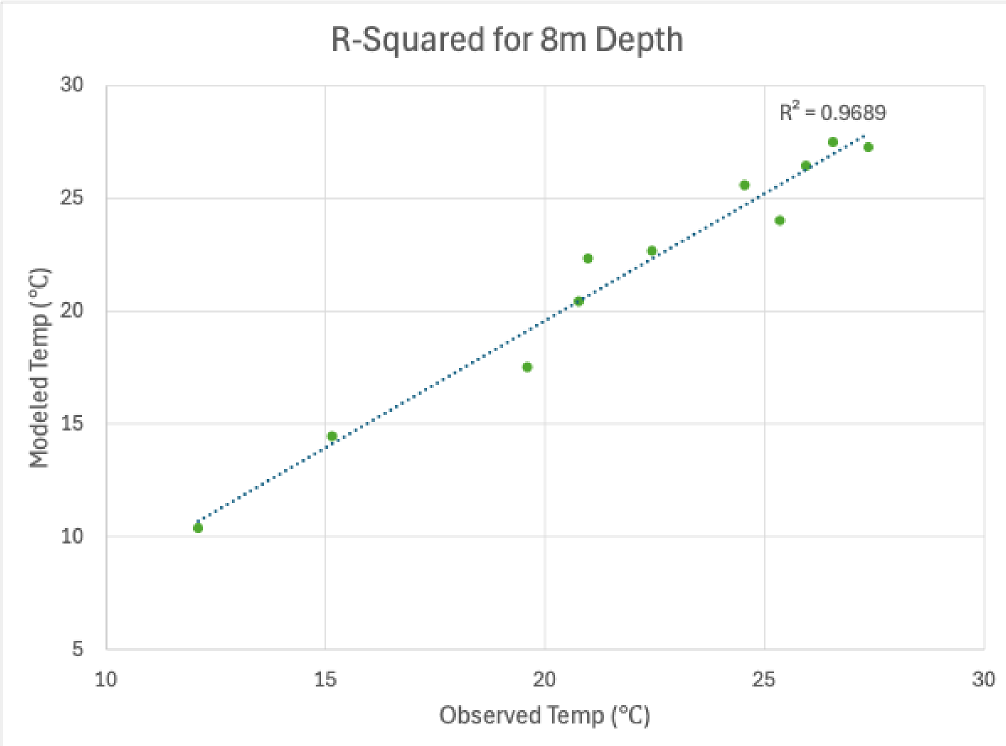

Appendix A Figure A.4 Observed vs modeled temperature at 8-m with R-squared.